Rerouting end-face-TIR capable rays to significantly increase evanescent wave signal power

Jianjun Ma[1*], Yasser Chiniforooshan[1], Huacai Chen[1,2], Jiahua Chen[1], Wojtek J. Bock[1], and Andrea Cusano[3]**

[1] *Centre de Recherche en Photonique, Département d'informatique et d'ingénierie, Université du Québec en Outaouais, Gatineau, Québec J8X 3X7, Canada*

[2] *College of Optical and Electronic Technology, China Jiliang University, Hangzhou 310018, China*

[3] *Optoelectronic Division, Engineering Department, University of Sannio, Benevento, Italy*

[*] *Corresponding author: ma.jianjun@uqo.ca;* [**] *corresponding author: huacaichen@cjlu.edu.cn*

Received December 9, 2010; accepted January 28, 2011; posted online March 25, 2011

The critical findings associated with end-face total internal reflection (TIR) phenomemon we proved before are reported. In particular, these findings reveal that the end-face-TIR capable rays experience enormous mode mixing when encountering a roughened end face. As a result, 94% of the overall detectable power is contributed by this effect. With a smooth fiber end face, this figure is mere 52%. We interpret the mechanism behind these unusual phenomena and its significance for the performance enhancement of fiber optic evanescent wave sensor.

OCIS codes: 060.2270, 060.2370, 300.6280.

doi: 10.3788/COL201109.040603.

A fiber optic evanescent wave (EW) sensing platform is a powerful tool to address the surface event that takes place within one wavelength thickness of the target sample. However, this advantage is often achieved at the cost of the optical signal level. Well-known measures to deal with this issue include a fiber taper[1], its modified form[2], and/or an extended interactive length between the fiber and the sample[3] that can vary from several centimeters to meters. Among other popular designs is the combination of positive→negative→positive fiber segments[4]. The requirement of mixing the sample with refractive index (RI) matching liquid to create the negative fiber segment obviously raises problems. Since some samples may not be readily compatible with the RI-matching liquid. A tapered fiber segment in the middle of a long fiber is also widely used[5]. Along with the fabrication difficulties involved, problems arise from double-bare tapers and a segment of thin glass cylinder sitting in between. The overall length is so long that fragility of the structure becomes a concern. A high-performance filter may also be required to block the likely strong excitation light from the light source. The overall sensing element size and fragility also pose questions to the U-shaped fiber-sensing segment[6].

In this letter, we present a new mechanism that may be able to provide a significant signal increase without resorting to a taper or a long fiber segment. This mechanism could also dramatically reduce the sample size to a mere liquid droplet as small as 2 mm in diameter.

As illustrated in Fig. 1, the BFL37-400 multimode fibers with core/cladding/jacket diameter of 400/430/730 μm and numerical aperture (NA) of 0.37 were used to establish a fiber optic EW sensing platform. This platform has a two-fiber architecture, with one fiber (illuminating fiber (i-fiber)) for excitation light delivery and the other for EW form fluorescent signal collection (receiving fiber (r-fiber)). The rhodamine 6G (R6G) diluted in water served as the representative of the fluorescence capable samples. The R6G was dispensed onto the r-fiber sidewall and covered the output end face of the i-fiber. The maximum fluorescent signal level was achieved by shaping the droplet via adjusting the two fibers to an optimum offset. This is indicated in the inset of Fig. 1. The associated mechanism for this optimum offset has been previously discussed[7]. A large RI-matching gel block was used when needed to eliminate any reflection at the fiber end face. An Ocean Optics USB 2000 palm-held spectrometer was connected with R-end for r-fiber via a SMA connector to monitor and record the fluorescent signal.

In our previous work[7,8], we demonstrated that only 9% of the overall fluorescent signal level arises from the right traveling power I_{F0}^{+}, as indicated in Fig. 1. In contrast, as high as 91% of the overall power was contributed by the left traveling power I_{F0}^{-} via the total internal reflection (TIR) occurring at the fiber S-end (end-face-TIR). This is in direct contradiction with the conventional wisdom. We interpret this phenomenon as the unique characteristic of high-order and tunneling modes that operate slightly above and just below cutoff, respectively, as previously described[8,9]. However, a question still remains: if the fiber end face is in a perfect condition, after experiencing the end-face-TIR, these rays should follow the same trajectories or preserve the same mode orders in terms of wave optics. Moreover, referring to Fig. 1 again, the end-face-TIR capable rays are affected by air, the liquid sample, and the polymer clad fiber segments before arriving at the R-end. The RIs of these materials are $n_{\mathrm{pl}} = 1.41$, $n_{\mathrm{liq}} = 1.33$, and $n_{\mathrm{air}} = 1$, respectively. Considering these values and $n_{\mathrm{co}} = 1.46$, the calculation based on our previous work[8] reveals that the end-face-TIR capable rays exist only in air- or liquid-clad fiber segment; they are inhibited by a polymer-clad segment. This leads to no

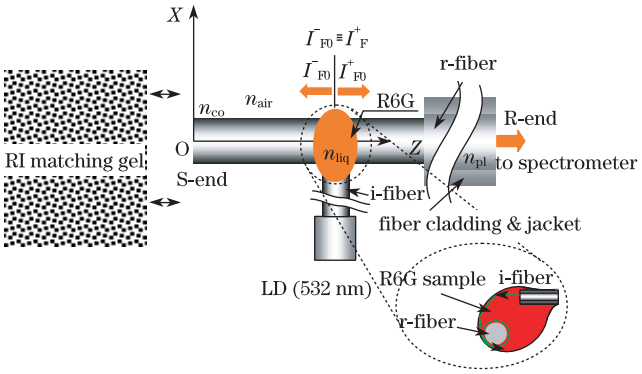

Fig. 1. Fiber optic EW sensing platform for the investigation of the end-face TIR and mode mixing effects on fluorescent signal level detected at the R-end.

observable signal rise at the R-end. Another conclusion holds for the end face at the R-end: if the R-end face is also roughened, all rays arriving at this end face exit via refraction rather than via reflection. This is true even after experiencing mode mixing because all rays allowed by the polymer-clad segment are not end-face-TIR capable.

In this letter, we provide solid experimental evidence and theoretical interpretation to this dilemma: the mechanism behind such a significant signal rise is the mode mixing originating from defects on the fiber end face. These defects reroute the trajectories of the end-face TIR rays and cause some of them to be detectable at the R-end.

In the experiment, two identical r-fibers with different S-end face conditions were prepared. One r-fiber has a roughened S-end face, generated by cutting the fiber end with a diamond tipped fiber optic scribe. Such treatment tends to produce significant defects at the end face of the chosen large core fiber. Under the microscope, defects were revealed as the combination of several slightly slanted flat surfaces and randomly chipped edges, as shown in Fig. 2(d). The S-end face of another r-fiber was prepared following a standard polishing process from coarse to fine sanding papers. This process provides a smooth end face with less pronounced surface defects, also shown in Fig. 2(d).

As expected and illustrated in Fig. 2(a), the roughened end face clearly assists in collecting much more fluorescent signal. This is approximately seven times higher than the level obtained in the case of the smooth end face.

Theoretically, we again conclude that defects distributed across the roughened fiber end face reroute the end-face-TIR capable rays upon reflection. When this occurs, the reflected rays do not follow their original trajectories. They merge into paths belonging to other rays, or other mode orders in terms of wave optics, causing the mode mixing effect to occur. Part of these merged modes fall into the mode category allowed by the adjacent polymer-clad fiber segment and become detectable at the R-end. In particular, power carried by these "merged modes" dominates the overall signal level because they receive the power from the end-face-TIR capable modes close to cutoff, which hold the strongest portion of signal power among all modes, as previously stated[8]. In contrast, power carried by the end-face-TIR capable modes directly traveling from R6G (associated with intensity, I_{F0}^{+} in Fig. 1) is blocked before entering the polymer-clad segment because it does not experience any mode mixing. To interpret this process more clearly, we look at Fig. 1. Only a segment of the air-clad fiber lies between the liquid- and polymer-clad segments. This segment is in fact a glass cylinder with a smooth sidewall surface and defect-free uniform internal material. As a result, when propagating along the liquid- and air-clad segments, all rays associated with I_{F0}^{+} are allowed because $n_{liq} > n_{air}$. No ray path changes or mode mixing occurs. Upon encountering the polymer-clad segment, however, only part of these rays are allowed to pass because of the condition of $n_{pl} > n_{liq}$. In particular, the blocked rays include all the end-face TIR rays because they already operate at close to cutoff condition for the liquid-clad segment. Upon encountering the polymer-clad segment, they become leaky rays and are quickly refracted out of the fiber. As a result, the impact of end-face TIR-capable rays associated with I_{F0}^{+} at the R-end is eliminated.

Further proofs strongly supporting the above argument are given by Figs. 2(b) and (c). Figure 2(b) shows that the fluorescent signal is mainly provided by the end-face-TIR rays. Thus, 94% of the overall signal level can be eliminated by simply applying a gel block to the rough fiber end face at the S-end, which cancels any end-face reflection effect. In comparison, Fig. 2(c) demonstrates that the gel causes only 52% of the signal drop for the smooth end face, implying a weaker mode mixing effect. Figure 2(d) illustrates the end-face conditions of the two fiber end faces associated with experimental results. Clearly, the end face treated with the

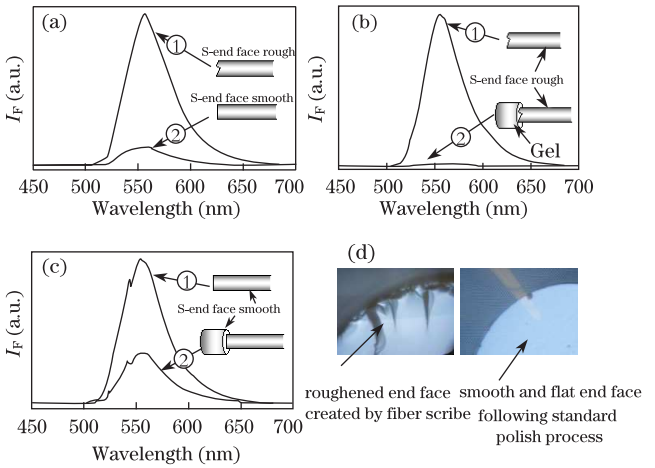

Fig. 2. Experimental evidence showing much stronger impact of the roughened end face on the fluorescent signal collection of the EW fiber optic sensing platform illustrated in Fig. 1. (a) The roughened endface introduces strong mode mixing; (b) for the rough end face, the elimination of the end-face TIR, and mode mixing significantly decreases the signal; (c) for the smooth end face presenting a weaker mode mixing, the same procedure as in (b) eliminates the signal on a much smaller scale. (d) Photo on the left: distribution of abundant defects on the outermost edge of the fiber S-end face generated using a diamond-tipped fiber scribe. Photo on the right: a nearly defect-free end face generated by the standard polishing process.

diamond-tipped fiber scribe generated a large amount of defects with a variety of sizes and shapes, most of which resided on the outmost edge of the end face. By noting that this is also the area occupied by the close to cutoff modes associated with the end-face-TIR rays, one can conclude that a significant scale of mode mixing will take place. In contrast, for the nearly defect-free end face and outmost edge, also shown in Fig. 2(d), the scale of mode mixing is minimized. All end-face-TIR rays are reflected back and followed their original paths. These are eventually blocked when encountering the polymer-clad fiber segment.

In conclusion, we have demonstrated the extraordinary scale of EW fluorescent signal rise triggered by the roughened fiber end face. Contrary to the traditional approach relying on the idea of increasing fiber length and/or using a taper for signal increase, the significance of this work lies in the fact that precious EW form signal can be enhanced by a fiber end face as small as 400 μm in diameter and a liquid sample droplet as tiny as few microliters. These findings pave the way towards a novel high-performance and low-cost EW sensor platform for a variety of chemical and biological sample analysis. In future investigations, we will optimize the defect distributions through theoretical modeling and experimental verifications to further increase the EW signal level. The obvious concern regarding the reproducibility of the defects will also be addressed by examining alternative technologies.

This work was supported by the Natural Science and Engineering Research Council of Canada, from Canada Research Chairs Program and from the Ministère de Développement Economique, Innovation et Exportation du Québec.

References

1. L. C. Shriver-lake, G. P. Anderson, J. P. Golden, and F. S. Ligler, Anal. Lett. **25,** 1183 (1992).
2. D. V. Lim, in *Proceedings of the IEEE* **91,** 902 (2003).
3. R. Orghici, U. Willer, M. Gierszewska, S. R. Waldvogel, and W. Schade, Appl. Phys. B **90,** 355 (2008).
4. M. Ahmad, K.-P. Chang, T. A. King, and L. L. Hench, Sensors and Actuators A **119,** 84 (2005).
5. P. Lucas, M. R. Riley, C. B. Pledel, and B. Bureau, Anal. Biochem. **351,** 1 (2006).
6. W. Cao and Y. Duan, Sensors and Actuators B **119,** 363 (2006).
7. J. Ma and W. J. Bock, Opt. Lett. **32,** 8 (2007).
8. J. Ma, W. J. Bock, and A. Cusano, Opt. Express **17,** 7630 (2009).
9. A. W. Snyder and J. D. Love, *Optical Waveguide Theory* (Springer, London, 1983).